

# Potential tumor-suppressive role of microRNA-99a-3p in sunitinib-resistant renal cell carcinoma cells through the regulation of *RRM2*

YOICHI OSAKO, HIROFUMI YOSHINO, TAKASHI SAKAGUCHI, SATOSHI SUGITA,  
MASAYA YONEMORI, MASAYUKI NAKAGAWA and HIDEKI ENOKIDA

Department of Urology, Graduate School of Medical and Dental Sciences,  
Kagoshima University, Kagoshima 890-8520, Japan

Received September 19, 2018; Accepted January 25, 2019

DOI: 10.3892/ijo.2019.4736

**Abstract.** Sunitinib is the most common primary molecular-targeted agent for metastatic clear cell renal cell carcinoma (ccRCC); however, intrinsic or acquired sunitinib resistance has become a significant problem in medical practice. The present study focused on microRNA (miR)-99a-3p, which was significantly downregulated in clinical sunitinib-resistant ccRCC tissues in previous screening analyses, and investigated the molecular network associated with it. The expression levels of miR-99a-3p and its candidate target genes were evaluated in RCC cells, including previously established sunitinib-resistant 786-o (SU-R-786-o) cells, and clinical ccRCC tissues, using reverse transcription-quantitative polymerase chain reaction. Gain-of-function studies demonstrated that miR-99a-3p significantly suppressed cell proliferation and colony formation in RCC cells, including the SU-R-786-o cells, by inducing apoptosis. Based on *in silico* analyses and RNA sequencing data, followed by luciferase reporter assays, ribonucleotide reductase regulatory subunit-M2 (*RRM2*) was identified as a direct target of miR-99a-3p in the SU-R-786-o cells. Loss-of-function studies using small interfering RNA against *RRM2* revealed that cell proliferation and colony growth were significantly inhibited via induction of apoptosis, particularly in the SU-R-786-o cells. Furthermore, the *RRM2* inhibitor Didox (3,4-dihydroxybenzohydroxamic acid) exhibited anticancer effects in the SU-R-786-o cells and other RCC cells. To the best of our knowledge, this is the first report demonstrating that miR-99a-3p directly regulates *RRM2*. Identifying novel genes targeted by tumor-suppressive miR-99a-3p in sunitinib-resistant RCC cells may improve our

understanding of intrinsic or acquired resistance and facilitate the development of novel therapeutic strategies.

## Introduction

Clear cell renal cell carcinoma (ccRCC) is the most common histological subtype of RCC, accounting for >70% of RCC (1). At the time of diagnosis, ~30% of patients have metastatic disease (2). Although surgical resection can effectively resolve ccRCC, 20-40% of patients continue to develop local recurrence or distinct metastasis following surgery (3,4). Molecular-targeted agents repressing the vascular endothelial growth factor (*VEGF*) or mammalian target of rapamycin (*mTOR*) genes have been routinely administered to patients with metastatic or recurrent RCC. Among these drugs, sunitinib is a common molecular-targeted agent that is recommended as a first-line therapy for patients with advanced RCC. Unfortunately, most patients treated with these drugs eventually suffer from progressive disease due to intrinsic or acquired resistance (5).

In a previous study, metabolic reprogramming was observed in sunitinib-resistant RCC cells, resulting in the acquisition of sunitinib resistance (6). In recent years, novel drugs have been developed as second-line treatments for advanced RCC. Nivolumab is an IgG4 antibody that causes immune checkpoint blockade by decreasing inhibitory signaling via the programmed death ligand-1 pathway (7). Nivolumab increases the overall survival (OS) time and is associated with decreased toxicity in comparison with everolimus according to the CheckMate 025 study (8). However, due to the high cost of nivolumab, it is necessary to define its usefulness from the viewpoint of efficacy as well as cost (9). Indeed, the phase 3 CheckMate 025 study demonstrated longer OS times with nivolumab compared with everolimus, but not significantly so. Additionally, the objective response rate of nivolumab-treated patients was only 25% (8). Therefore, it is necessary to identify novel therapeutic modalities to defeat sunitinib resistance.

MicroRNAs (miRNAs/miRs) are a class of small noncoding RNAs (~22 nucleotides) that have roles in the inhibition or degradation of target RNA transcripts in a sequence-dependent manner (10). Numerous miRNAs

---

*Correspondence to:* Dr Hideki Enokida, Department of Urology, Graduate School of Medical and Dental Sciences, Kagoshima University, 8-35-1 Sakuragaoka, Kagoshima 890-8520, Japan  
E-mail: enokida@m.kufm.kagoshima-u.ac.jp

**Key words:** microRNA-99a-3p, ribonucleotide reductase regulatory subunit-M2, sunitinib resistance, renal cell carcinoma, Didox

have tissue-specific expression (11), and >2,000 different miRNAs have been identified in humans (12). miRNAs are abnormally expressed in several human cancer types, and certain miRNAs are frequently downregulated in numerous types of cancer (13-15), suggesting that they function as tumor suppressors by targeting multiple oncogenes. Several studies have demonstrated that modulating miRNA expression levels can increase the efficacy of chemotherapy (16,17). Furthermore, silencing multiple genes using a single miRNA can simultaneously control several signaling pathways and minimize compensatory mechanisms that cause therapeutic resistance (18). miRNAs have also been reported to be associated with sunitinib resistance. For example, miR-144-3p mediates sunitinib resistance by targeting the AT-rich interactive domain 1A gene in ccRCC (19). Therefore, miRNAs may represent promising candidates for the treatment of RCC in patients with intrinsic or acquired resistance to sunitinib.

Accordingly, the aim of the present study was to investigate the functional importance of miR-99a-3p and to discover the molecular targets that are regulated by this miRNA in sunitinib-resistant RCC. Gain-of-function studies were performed in miR-99a-3p transfectants and novel miR-99a-3p-mediated molecular targets and pathways were investigated through *in silico* analysis and RNA sequencing. The discovery that miR-99a-3p regulates targets and pathways may provide novel insights into the mechanisms of intrinsic or acquired resistance to sunitinib.

## Materials and methods

**Clinical tissues and human RCC cell lines.** ccRCC and normal adjacent kidney tissues were collected from 40 patients who sequentially underwent radical or partial nephrectomy at Kagoshima University Hospital (Kagoshima, Japan) between 2005 and 2010 (Table I). The stage and grade of the samples were determined according to the American Joint Committee on Cancer/International Union Against Cancer classification and histologically graded (20) at the Department of Veterinary Histopathology of Kagoshima University. The samples were kept in RNAlater™ (Thermo Fisher Scientific, Inc., Waltham, MA, USA) at -20°C until RNA extraction. The present study was approved by the Bioethics Committee of Kagoshima University, and written informed consent and was obtained from all patients.

Human RCC cells (786-o, A498, ACHN, Caki1, and Caki2 cells) were purchased from the American Type Culture Collection (ATCC, Manassas, VA, USA). The sunitinib-resistant 786-o (SU-R-786-o) cell line was previously established by administration of sunitinib to mice (6).

**Cell culture and RNA extraction.** Cells were cultured in RPMI-1640 medium (Invitrogen; Thermo Fisher Scientific, Inc.) with 10% fetal bovine serum and kept in a humidified incubator (5% CO<sub>2</sub>) at 37°C. Routine tests for mycoplasma infection were negative. Total RNA, including the miRNA and the mRNA fractions, was extracted using a mir-Vana miRNA Isolation kit (Thermo Fisher Scientific, Inc.) according to the manufacturer's protocol. The quality of the RNA was tested using an RNA 6000 Nano assay kit and a 2100 Bioanalyzer (both Agilent Technologies, Inc., Santa Clara, CA, USA).

Table I. Patient characteristics (n=40).

Characteristic	Value
Median age (range), years	66.5 (41-89)
Sex, n (%)	
Male	28 (70.0)
Female	12 (30.0)
Pathological tumor stage <sup>a</sup> , n (%)	
pT1a	20 (50.0)
pT1b	13 (32.5)
pT2	0 (0.0)
pT3a	4 (10.0)
pT3b	3 (7.5)
pT4	0 (0.0)
Tumor grade <sup>a</sup> , n (%)	
G1	3 (7.5)
G2	30 (75.0)
G3	6 (15.0)
N/A	1 (2.5)
Metastasis <sup>a</sup> , n (%)	
M 0	36 (90.0)
M 1	2 (5.0)
N/A	2 (5.0)
Venous invasion <sup>a</sup> , n (%)	
v 1	25 (62.5)
v 0	15 (37.5)

<sup>a</sup>The stage and grade of the samples were determined according to the American Joint Committee on Cancer/International Union Against Cancer classification (17).

Human kidney total RNA (cat. no. AM7976; Thermo Fisher Scientific, Inc.) was used as normal kidney control RNA.

**Reverse transcription-quantitative polymerase chain reaction (RT-qPCR).** Stem-loop RT-qPCR (TaqMan MicroRNA Assays; Assay ID: 002141 for miR-99a-3p; Applied Biosystems; Thermo Fisher Scientific, Inc.) was employed to quantify miRNA following the manufacturer's protocol. Human *RNU48* (P/N: 001006; Applied Biosystems; Thermo Fisher Scientific, Inc.) was used as an internal control, and the 2<sup>-ΔΔC<sub>q</sub></sup> method was used to calculate the relative changes (21). For ribonucleotide reductase regulatory subunit-M2 (*RRM2*), SYBR-Green qPCR was performed, and the primer sequences are listed in Table II. Briefly, 500 ng total RNA was reverse transcribed into cDNA using the High Capacity cDNA Reverse Transcription kit (Thermo Fisher Scientific, Inc.) under the incubation conditions of 25°C for 10 min, 37°C for 120 min and 85°C for 5 min. qPCR was performed using a Power SYBR Green Master Mix (cat. no. 4367659) on a 7300 Real-time PCR System (both Applied Biosystems; Thermo Fisher Scientific, Inc.). The thermocycling protocol used was as follows: Initial activation step at 95°C for 10 min, followed by 40 cycles of a denaturation step at 95°C for 15 sec and an annealing/extension step at 60°C for 1 min. The amplification

Table II. Sequences of the primers used in the present study.

Gene	Forward (3'-5')	Reverse (3'-5')
<i>GUSB</i>	CGTCCCACCTAGAATCTGCT	TTGCTCACAAAGGTCACAGG
<i>RRM2</i>	CACGGAGCCGAAAATAAGC	TCTGCCTTCTTATACATCTGCCA
<i>MKI67</i>	ACGCCTGGTTACTATCAAAAGG	CAGACCCATTACTTGTGTTGGA
<i>PPP6R1</i>	TGACCTGCACACAAGCTCG	GGTTGACGACCTTGCACTC
<i>PLXNA1</i>	ACCCACCTAGTGGTGCCTC	CGGTTAGCGGCATAGTCCA

GUSB, glucuronidase  $\beta$ ; RRM2, ribonucleotide reductase regulatory subunit-M2; MKI67, proliferation marker Ki-67; PPP6R1, serine/threonine-protein phosphatase 6 regulatory subunit 1; PLXNA1, plexin-A1.

Table III. Sequences of the miRNA mimics used in the present study.

miRNA	Mature accession no. <sup>a</sup>	Sequence (5'-3')
let-7c-5p	MIMAT0000064	UGAGGUAGUAGGUUGUAUGGUU
miR-1-3p	MIMAT0000416	UGGAAUGUAAAGAAGUAUGUAU
miR-135-5p	MIMAT0000428	UAUGGCUUUUUAUCCUAUGUGA
miR-144-3p	MIMAT0000436	UACAGUAUAGAUGAUGUACU
miR-204-5p	MIMAT0000265	UCCCCUUGUCAUCCUAUGCCU
miR-23b-3p	MIMAT0000418	AUCACAUUGCCAGGGAAUACCAC
miR-26b-5p	MIMAT0000083	UUCAAGUAAUUCAGGAUAGGU
miR-27b-3p	MIMAT0000419	UUCACAGUGGCUAAGUUCUGC
miR-29b-3p	MIMAT0000100	UAGCACCAUUUGAAAUCAGUGUU
miR-29c-3p	MIMAT0000681	UAGCACCAUUUGAAAUCGGUUA
miR-30a-5p	MIMAT0000087	UGUAAACAUCUCGACUGGAAG
miR-31-3p	MIMAT0004504	UGCUAUGCCAACAUAUUGCCAU
miR-429	MIMAT0001536	UAAUACUGUCUGGUAAAACCGU
miR-766-3p	MIMAT0003888	ACUCCAGCCCCACAGCCUCAGC
miR-99a-3p	MIMAT0024017	ACCCACCTAGTGGTGCCTC

<sup>a</sup>From the miRbase database (<http://www.mirbase.org/>) (12). miRNA/miR, microRNA.

specificity was confirmed by monitoring the dissociation curve of the amplified product. All expression data were normalized to the glucuronidase  $\beta$  gene, and the  $2^{-\Delta\Delta C_q}$  method was employed to calculate the relative changes.

**Transfection with miRNA mimic and small interfering (si)RNA into RCC and SU-R-786-o cells.** As described previously (22), ACHN, 786-o and SU-R-786-o cells were transfected using Lipofectamine<sup>TM</sup> RNAiMAX transfection reagent and Opti-MEM (both Thermo Fisher Scientific, Inc.) containing 10 nM mature miRNA or RRM2 siRNA. Mature miRNAs and pre-miR miRNA precursors (*hsa-miR-99a-3p*; product ID, PM12983; negative control miRNA product ID, AM17111) were employed for the gain-of-function experiments, whereas RRM2 siRNA (product ID, HSS109390 and HSS109392) and negative control siRNA (product ID, D-001810-10) (all Thermo Fisher Scientific, Inc.) were employed for the loss-of-function experiments. The sequences of all miRNA mimics and siRNAs are listed in Tables III and IV. Different negative controls (miRNA/siRNA) were used for each cancer cell line to prevent

off-target effects. The optimization of the transfection efficacy of the microRNA precursors in the RCC cell lines was based on the downregulation of *PTK9* mRNA by over-expression of miR-1, as recommended by the manufacturer (Thermo Fisher Scientific, Inc.). The transfection efficiency of all miRNA mimics was evaluated accordingly. In order to establish the RRM2 siRNA transfection efficacy, RT-qPCR and western blot analyses were performed to confirm the downregulation of *RRM2* mRNA and protein levels.

**Cell proliferation, colony formation, apoptosis and cell cycle assays, and determination of half maximal inhibitory concentration ( $IC_{50}$ ) values.** To investigate the functional importance of miR-99a-3p and *RRM2*, cell proliferation, colony formation and apoptosis assays were performed using ACHN, 786-o, and SU-R-786-o cells. Didox (3,4-dihydroxybenzohydroxamic acid; Cayman Chemical Company, Ann Arbor, MI, USA) was used as an RRM2 inhibitor. The cell proliferation was examined 72 h after transfection using XTT assays (Roche Applied Science,

Table IV. Sequences of the siRNAs used in the present study.

siRNA	Cat. no.	Directionality	Sequence (5'-3')
si-RRM2_1	10620318	Sense	GCCUGAUGUCAAACACCUUGGUACA
	10620319	Antisense	UGUACCAGGUGUUUGAACAUCAAGGC
si-RRM2_2	10620318	Sense	ACCAUGAUUUCUGGCAGAUUAUAA
	10620319	Antisense	UUAUACAUCUGCCAGAUUAUCAUGGU

siRNA, small interfering RNA.

Penzberg, Germany), according to the manufacturer's instructions. For the colony formation assays, 1,000 cells were plated into 10-cm dishes following transfection for 10 days to confirm optimal colony formation, followed by staining with 0.04% crystal violet (Nacalai Tesque, Inc., Kyoto, Japan) at room temperature for 10 min. The cell cycle and apoptosis assays were performed by flow cytometry (CytoFLEX Analyzer; Beckman Coulter, Inc., Brea, CA, USA) using a Cycletest PLUS DNA Reagent kit and FITC Annexin V Apoptosis Detection kit (both BD Biosciences, San Jose, CA, USA), respectively, following the manufacturer's protocols (23). Cell viability was assessed using an XTT cell proliferation assay kit. The IC<sub>50</sub> values of sunitinib were assessed in accordance with the relative survival curve.

**Plasmid construction and dual-luciferase reporter assay.** Partial wild-type sequences of the 3'-untranslated region (UTR) of *RRM2* or those with a deleted miR-99a-3p target site were inserted between the *Xho*I and *Pme*I restriction sites in the 3'-UTR of the hRluc gene in a psiCHECK-2 vector (C8021; Promega Corporation, Madison, WI, USA). ACHN, 786-o, and SU-R-786-o cells were transfected with 50 ng vector and 10 nM miR-99a-3p. The activities of firefly and Renilla luciferases in cell lysates were recorded. The procedure for the dual-luciferase reporter assays was described previously (24).

**Western blotting.** The cells were harvested 72 h after transfection and total protein lysate was prepared with a radioimmunoprecipitation assay buffer (Thermo Fisher Scientific, Inc.) containing a protease inhibitor cocktail (Sigma-Aldrich; Merck KGaA, Darmstadt, Germany). The protein concentrations were determined using the Bradford assay (25). Protein lysates (50 µg) were separated on NuPAGE 4-12% Bis-tris gels (Invitrogen; Thermo Fisher Scientific, Inc.) and transferred to polyvinylidene difluoride membranes. Immunoblotting was performed with diluted rabbit polyclonal anti-RRM2 antibodies (1:500; cat. no. 11661-1-AP; Proteintech Group, Inc., Chicago, IL, USA), rabbit polyclonal anti-poly(ADP-ribose) polymerase (PARP) antibodies (1:500; cat. no. 9542), rabbit monoclonal anti-cleaved PARP antibodies (1:500; cat. no. 5625) (both Cell Signaling Technology, Inc., Danvers, MA, USA), and rabbit polyclonal anti-β-actin antibodies (1:5,000; cat. no. bs-0061R; Bioss, Beijing, China). Specific complexes were visualized using an echoluminescence detection system (GE Healthcare Life Sciences, Little Chalfont, UK) as described previously (26).

**In silico analysis for identifying genes regulated by miR-99a-3p.** *In silico* analysis was used to identify genes targeted by miR-99a-3p. To obtain candidate target genes regulated by miR-99a-3p, TargetScan database Release 7.1 (<http://www.targetscan.org>) was used. Additionally, the Gene Expression Omnibus (GEO) database (accession nos. GSE36895 and GSE22541; <https://www.ncbi.nlm.nih.gov/geo/>) was employed to identify upregulated genes in ccRCC tissues.

**Bioinformatics analysis.** In order to evaluate the clinical relevance, The Cancer Genome Atlas (TCGA) cohort database of 534 patients with ccRCC was used. Full sequencing and clinical information were obtained through University of California Santa Cruz Xena (<http://xena.ucsc.edu/>), cBioPortal for Cancer Genomics (<http://www.cbioportal.org/public-portal/>), and TCGA (<https://tcga-data.nci.nih.gov/tcga/>). The present study met the criteria for the publication guidelines provided by TCGA (<http://cancergenome.nih.gov/publications/publicationguidelines>).

**Statistical analysis.** The statistical comparisons between two or three variables and numerical values were analyzed by Mann-Whitney U tests and Bonferroni-adjusted Mann-Whitney U tests, respectively. All experiments were performed in triplicate. Spearman's rank tests were used to evaluate the correlation between the expression of miR-99a-3p and *RRM2*. Kaplan-Meier and log-rank methods were used to analyze the associations between miR-99a-3p and candidate target genes, including *RRM2*, and OS time by using the OncoLnc dataset (<http://www.oncolnc.org/>), which contains survival data for 8,647 patients from 21 cancer studies performed by TCGA. OncoLnc is a useful tool for exploring survival correlations, and for downloading clinical data coupled to expression data for mRNAs, miRNAs or long noncoding RNAs as previously described (27). All analyses were performed on Expert StatView software version 5.0 (SAS Institute, Inc., Cary, NC, USA). P<0.05 was considered to indicate statistically significant differences.

## Results

**Identification of miRNAs that exhibit decreased expression in sunitinib-resistant RCC.** Initially, 15 miRNAs that exhibited decreased expression and had not been previously analyzed in sunitinib-resistant RCC were selected (28-31) (Table III). XTT assays were performed using 786-o and SU-R-786-o cells transfected with these 15 miRNAs in order to select candidate



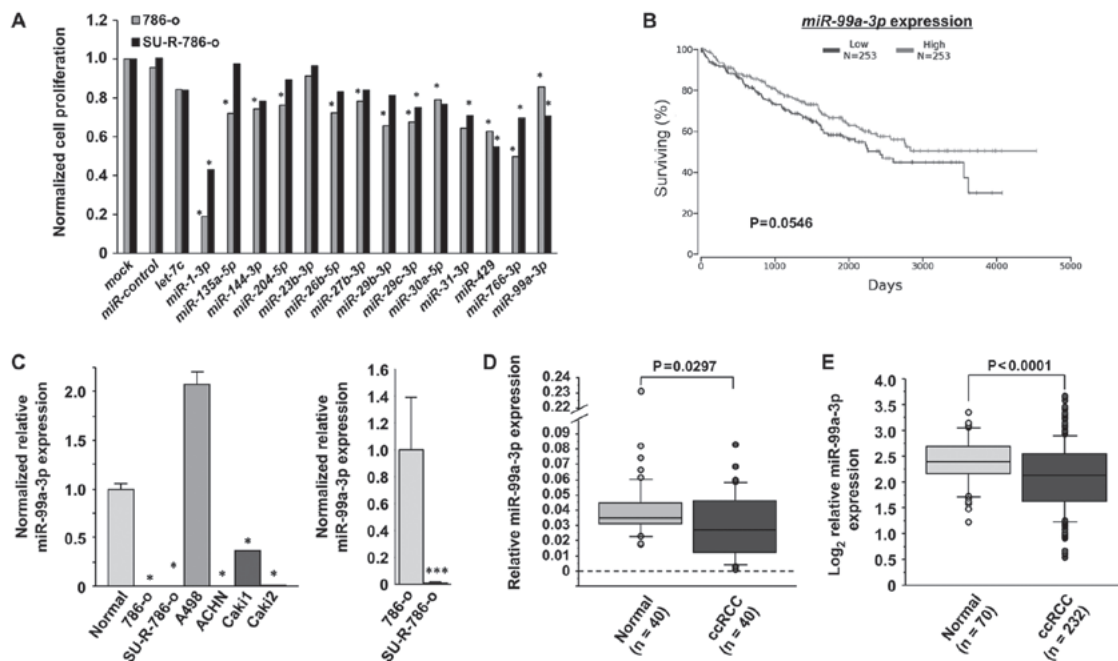


Figure 1. Clinical significance and expression levels of miR-99a-3p in RCC. (A) Cell proliferation was examined by XTT assays 72 h after transfection with 10 nM miRNAs in 786-o and SU-R-786-o cells in order to select candidate miRNAs. Significant cell proliferation inhibition was observed in the two cell types transfected with the following miRNAs: miR-1-3p, miR-29c-3p, miR-429, miR-766-3p and miR-99a-3p. \* $P<0.0001$  versus miR-control. (B) Analysis of a ccRCC cohort from TCGA in OncoLnc revealed longer OS times in the patients with high miR-99a-3p expression ( $n=253$ ) in comparison with those with low expression ( $n=253$ ), but the difference was not statistically significant ( $P=0.0546$ ). (C) The expression levels of miR-99a-3p were significantly lower in 4 RCC cell lines (786-o, ACHN, Caki1 and Caki2) and in SU-R-786-o cells than those in normal kidney cells. The expression levels of miR-99a-3p in SU-R-786-o cells were lower than those in 786-o cells. \* $P<0.0001$  vs. normal; \*\*\* $P<0.05$  vs. 786-o. (D) The miR-99a-3p levels were lower in clinical ccRCC tissues ( $n=40$ ) compared with their adjacent noncancerous tissues ( $n=40$ ) ( $P=0.0297$ ). (E) In a dataset obtained from TCGA, miR-99a-3p expression was significantly downregulated in ccRCC samples ( $n=232$ ) compared with that in normal samples ( $n=70$ ) ( $P<0.001$ ). RCC, renal cell carcinoma; ccRCC, clear cell RCC; miR/miRNA, microRNA; TCGA, The Cancer Genome Atlas.

miRNAs (Fig. 1A). The results revealed that 5 miRNA transfectants (miR-1-3p, miR-29c-3p, miR-429, miR-766-3p and miR-99a-3p) inhibited cell proliferation in comparison with miR-control. Additionally, among these 5 miRNAs, the OncoLnc analysis revealed a trend towards longer OS times in the patients with high miR-99a-3p expression ( $n=253$ ) compared with those in the patients with low expression ( $n=253$ ) in the TCGA ccRCC cohort, but this was not statistically significant ( $P=0.0546$ ; Fig. 1B). Therefore, miR-99a-3p was chosen for further analyses.

**miR-99a-3p expression in RCC cell lines, SU-R-786-o cells, and ccRCC clinical tissues.** The expression levels of miR-99a-3p were examined in clinical ccRCC tissues ( $n=40$ ), their adjacent noncancerous tissues ( $n=40$ ), RCC cell lines and SU-R-786-o cells by RT-qPCR. The miR-99a-3p levels were significantly lower in four of the RCC cell lines (786-o, ACHN, Caki1 and Caki2) and in SU-R-786-o cells than in normal kidney cells ( $P<0.0001$ ; Fig. 1C). Notably, the expression levels in the SU-R-786-o cells were lower than those in the parental 786-o cells ( $P=0.0495$ ). Furthermore, miR-99a-3p revealed lower expression in the clinical ccRCC specimens compared with their adjacent noncancerous tissues ( $P=0.0297$ ; Fig. 1D). The clinicopathological information of the patients is listed in Table I. No significant associations were observed between any of the clinicopathological parameters and miR-99a-3p expression in this cohort (data not shown). In addition, within the ccRCC dataset from TCGA, the expression level of

miR-99a-3p was significantly downregulated in patients with ccRCC ( $n=232$ ) compared with that in healthy patients ( $n=70$ ;  $P<0.0001$ ; Fig. 1E). These data imply that miR-99a-3p may be a potential therapeutic target in RCC and sunitinib-resistant RCC cells.

**Effects of restoring miR-99a-3p expression on cell proliferation, apoptosis, cell cycle and colony formation in RCC cell lines and SU-R-786-o cells.** In order to investigate the functional roles of miR-99a-3p, gain-of-function studies were performed using miRNA-transfected ACHN, 786-o and SU-R-786-o cells. Using XTT assays, miR-99a-3p overexpression was revealed to significantly suppress cell proliferation in comparison with the mock or miR-control transfectants ( $P<0.0001$ ; Fig. 2A). As miR-99a-3p transfection significantly inhibited cell proliferation in SU-R-786-o and other RCC cells, it was hypothesized that this miRNA may induce cell apoptosis. Hence, flow cytometric analyses were performed to count the number of apoptotic cells following the restoration of miR-99a-3p expression. The number of apoptotic cells (apoptotic and early apoptotic cells) was significantly higher in miR-99a-3p-transfected SU-R-786-o cells than in the mock or miR-control transfectants ( $P<0.0001$ ; Fig. 2B). Similarly, in the ACHN and 786-O cells, the miR-99a-3p transfectants exhibited increased apoptosis in comparison with the controls ( $P<0.0001$ ; Fig. 2B). Western blot analyses demonstrated that the expression of cleaved PARP was markedly increased in the miR-99a-3p transfectants compared with that in the

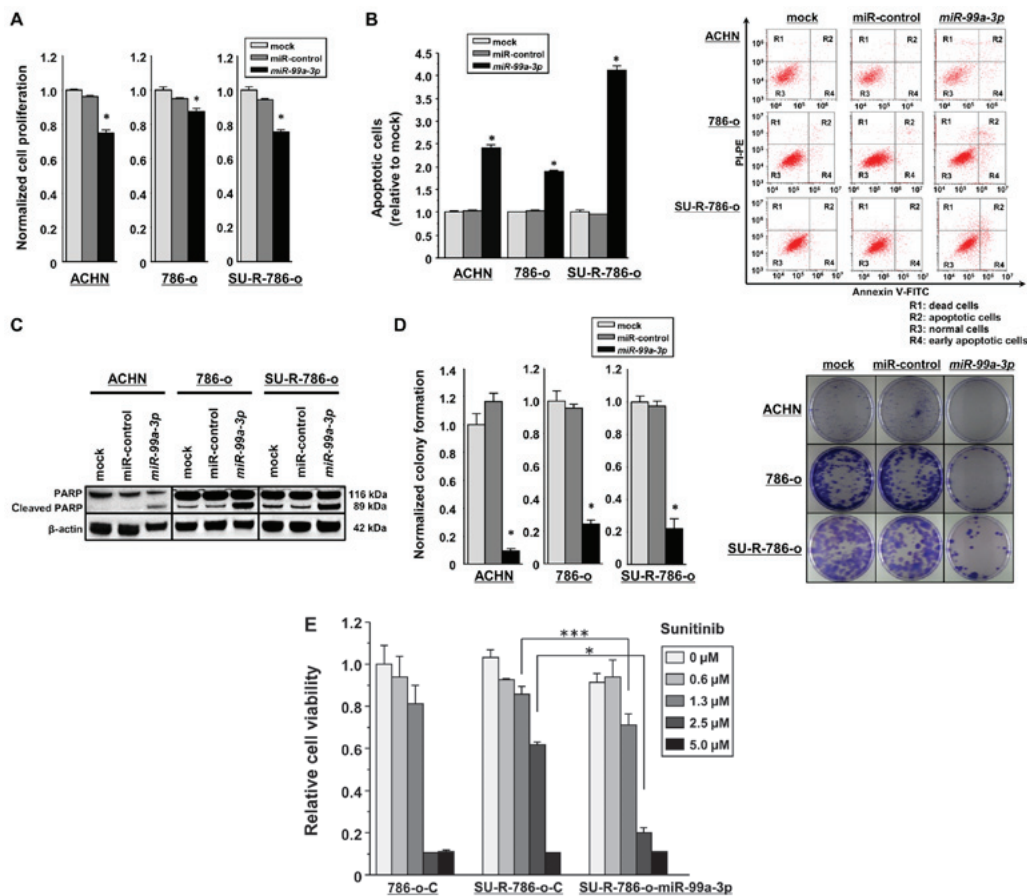


Figure 2. Functional analysis of miR-99a-3p. (A) Cell proliferation was examined by XTT assays 72 h after transfection with 10 nM miR-99a-3p. \* $P < 0.0001$ . (B) Apoptosis assays were performed using flow cytometry. Early apoptotic cells are plotted in the R4 quadrant and apoptotic cells are plotted in the R2 quadrant (right panel). The normalized ratios of apoptotic cells are plotted in the histogram (left panel). \* $P < 0.0001$ . (C) Western blot analysis of apoptotic marker cleaved PARP in ACHN, 786-o and SU-R-786-o cells.  $\beta$ -actin was employed as a loading control. (D) Colony formation was inhibited in the cells transfected with miR-99a-3p compared with that in the mock or miR-control groups. \* $P < 0.0001$ . (E) Cell viability following treatment with increasing sunitinib concentrations (0.6, 1.3, 2.5 and 5.0  $\mu$ M) was measured using the XTT assay. Sunitinib sensitivity was increased in SU-R-786-o transfected with miR-99a-3p compared with that in the same cells transfected with miR-control. \* $P < 0.0001$  and \*\*\* $P < 0.05$ . miR, microRNA; PARP, poly(ADP-ribose) polymerase; SU-R-786-o-miR-99a-3p, SU-R-786-o cells transfected with miR-99a-3p; SU-R-786-o-C, SU-R-786-o cells transfected with miR-control; FITC, fluorescein isothiocyanate.

controls (Fig. 2C). The cell cycle effects were also investigated using miR-99a-3p-transfected 786-o and SU-R-786-o cells. Overexpression of miR-99a-3p induced S-phase arrest in the two cell types (Fig. S1). In addition, colony formation assays using SU-R-786-o, ACHN, and 786-o cells revealed significantly decreased colony numbers in miR-99a-3p transfectants compared with those in the mock or miR-control transfectants (Fig. 2D). Furthermore, cell viability assays were performed using SU-R-786-o cells treated with various concentrations of sunitinib, and the viability of the cells was assessed with XTT assays (Fig. 2E). Notably, sunitinib sensitivity was restored in miR-99a-3p-transfected SU-R-786-o cells; the sunitinib  $IC_{50}$  values were 3.04, 1.72 and 1.38  $\mu$ M in the SU-R-786-o cells transfected with miR-control, those transfected with miR-99a-3p, and the parental 786-o cells, respectively. These results suggest that miR-99a-3p may function as a tumor suppressor in SU-R-786-o and other RCC cells.

**Identification of the *RRM2* gene as a target for miR-99a-3p in SU-R-786-o cells.** In order to gain further insights into the molecular mechanisms and pathways associated with the tumor-suppressing functions of miR-99a-3p in SU-R-786-o cells, a combination of *in silico* analyses and RNA sequencing

were performed on SU-R-786-o cells. Fig. 3A indicates the method of narrowing down the genes targeted by miR-99a-3p. The candidate target genes were identified using *in silico* analyses including TargetScan database Release 7.1 and the GEO database (accession nos. GSE36895 and GSE22541). Overall, 1,592 candidate target genes were selected that had  $\geq 1$  target sites. Additionally, from the GEO database, 12,831 genes were significantly upregulated in clinical ccRCC tissues in comparison with normal kidney tissues. RNA sequencing expression analysis was applied to identify the genes significantly upregulated in SU-R-786-o cells compared with the parental 786-o cells, and 16 candidate target genes were selected. Among these, 4 genes [*RRM2*, proliferation marker Ki-67 (*MKI67*), serine/threonine-protein phosphatase 6 regulatory subunit 1 (*PPP6R1*) and plexin-A1 (*PLXNA1*)] were chosen that were associated with significant differences in OS time, as revealed by Kaplan-Meier analysis of TCGA ccRCC cohort using the OncoLnc dataset (Figs. 3B and S2). Of these 4 candidate genes, *RRM2* was investigated due to its knockdown efficiency being higher than that of the other 3 genes in miR-99a-3p-transfected SU-R-786-o cells than in the mock or miR-control transfectants (Fig. S3). Furthermore, the *RRM2* expression levels in RCC cell lines were examined by

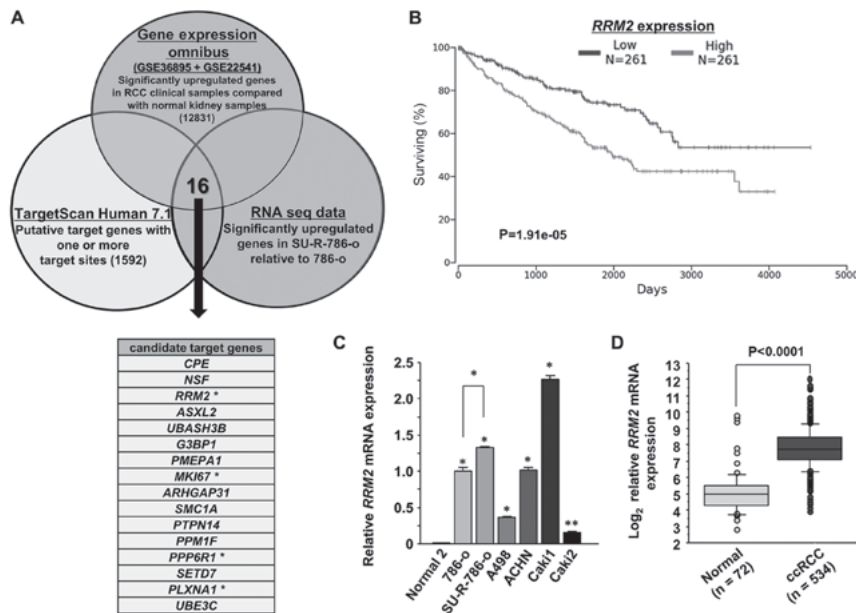


Figure 3. Identification of *RRM2* as a candidate miR-99a-3p target gene. (A) Venn diagram of the results from RNA sequencing and *in silico* analyses indicated 16 putative candidate target genes as key factors in SU-R-786-o cells. Four genes, *RRM2*, *MKI67*, *PPP6R1* and *PLXNA1*, were linked to significant differences in OS rates by Kaplan-Meier analysis of ccRCC cohort from TCGA. (B) Kaplan-Meier analysis demonstrated that the group of patients with high *RRM2* expression (n=261) exhibited lower OS rates compared with those in the low expression group in the OncoLnc dataset (n=261) ( $P<0.0001$ ). (C) The mRNA expression levels of *RRM2* were examined in RCC cell lines by reverse transcription-quantitative polymerase chain reaction. The expression levels were significantly upregulated in RCC cells in comparison with those in normal kidney cells. *RRM2* expression in SU-R-786-o cells was significantly higher than that in 786-o cells. \* $P<0.0001$  and \*\* $P<0.001$ . (D) The mRNA levels of *RRM2* were significantly upregulated in the ccRCC samples of TCGA dataset (n=534) compared with those in the normal samples (n=72). ( $P<0.0001$ ). *RRM2*, ribonucleotide reductase regulatory subunit-M2; *MKI67*, proliferation marker Ki-67; *PPP6R1*, serine/threonine-protein phosphatase 6 regulatory subunit 1; *PLXNA1*, plexin-A1; miR, microRNA; OS, overall survival; TCGA, The Cancer Genome Atlas.

RT-qPCR. *RRM2* was revealed to be significantly upregulated in all tested RCC cell lines compared with RNA from normal kidneys (Fig. 3C). Notably, *RRM2* expression in SU-R-786-o cells was significantly upregulated in comparison with that in parental 786-o cells ( $P<0.0001$ ). Additionally, it was upregulated in patients with ccRCC (n=534) compared with healthy individuals (n=72) in the ccRCC cohort from TCGA database ( $P<0.0001$ ; Fig. 3D).

*RRM2 is directly targeted by miR-99a-3p in SU-R-786-o cells.* RT-qPCR and western blot analyses were performed to confirm that overexpression of miR-99a-3p resulted in downregulation of *RRM2* in ACHN, 786-o and SU-R-786-o cells. *RRM2* mRNA and protein levels were significantly decreased in miR-99a-3p transfectants compared with those in the mock or miR-control transfectants (Fig. 4A and B). Dual luciferase reporter assays were performed to examine whether the *RRM2* gene was regulated through direct interaction by miR-99a-3p. The TargetScan database predicted a binding site for miR-99a-3p in the 3'-UTR of *RRM2* (positions 258-274). Vectors encoding the partial wild-type sequence of the 3'-UTR of *RRM2* were employed, including the predicted miR-99a-3p target sites. The luminescence intensity was significantly diminished in the case of co-transfection with miR-99a-3p and the vector carrying the wild-type 3'-UTR. In contrast, no decrease in luminescence was observed following transfection with the binding site deletion vector ( $P<0.0001$ ; Fig. 4C). Furthermore, the relationship between miR-99a-3p and *RRM2* expression levels in clinical ccRCC tissues was investigated using TCGA database. A significant negative correlation was

revealed between miR-99a-3p and *RRM2* mRNA expression according to Spearman's rank test ( $P=0.0011$ ,  $R=-0.189$ ; Fig. 4D). These results suggest that miR-99a-3p directly binds to specific sites at positions 258-274 of the *RRM2* 3'-UTR.

*Effects of RRM2 knockdown on cell proliferation, apoptosis, cell cycle and colony formation in SU-R-786-o cells.* In order to investigate the functional role of *RRM2* in SU-R-786-o cells, loss-of-function assays were conducted using si-*RRM2*. The knockdown efficacies of si-*RRM2* transfection were examined in ACHN, 786-o and SU-R-786-o cells. In the present study, two siRNAs targeting *RRM2* were employed (si-*RRM2*\_1 and si-*RRM2*\_2). RT-qPCR and western blot analyses indicated that these siRNAs effectively downregulated *RRM2* mRNA and protein expression in ACHN, 786-o and SU-R-786-o cells ( $P<0.0001$ ; Fig. 5A and B). XTT assays demonstrated that cell proliferation was inhibited in the si-*RRM2* transfectants in comparison with that in the mock or si-control transfectants (Fig. 5C). In the apoptosis assays, the number of apoptotic cells was significantly greater in the si-*RRM2* transfectants than in the controls (Fig. 5D). Western blot analyses demonstrated that the levels of cleaved PARP were markedly increased when *RRM2* was silenced (Fig. 5E). The cell cycle assays revealed that S-phase arrest was induced in the si-*RRM2* transfected 786-o cells, whereas *RRM2* knockdown in the SU-R-786-o cells increased the fraction of cells in the  $G_0/G_1$  phase (Fig. S1). Furthermore, colony formation assays confirmed that the development of colonies was significantly suppressed in the *RRM2*-knockdown RCC cells, including SU-R-786-o cells, compared with that in the controls (Fig. 5F). These results



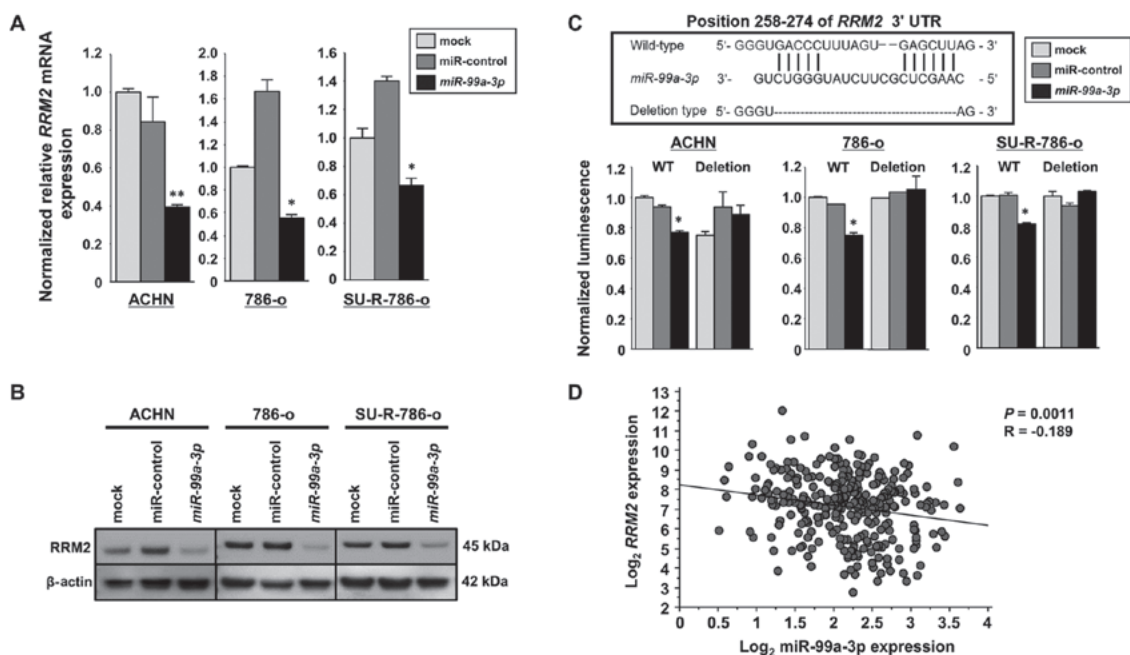


Figure 4. Direct targeting of *RRM2* by miR-99a-3p. (A) The expression of *RRM2* was significantly inhibited in the cells transfected with miR-99a-3p compared with that in the mock and miR-control groups. *GUSB* was employed as an internal control. \* $P < 0.0001$  and \*\* $P < 0.001$  versus the mock and miR-control groups. (B) The expression of *RRM2* protein was significantly inhibited in the miR-99a-3p transfectants compared with that in the mock or miR-control groups.  $\beta$ -actin was employed as a loading control. (C) Dual-luciferase reporter assays using vectors encoding putative miRNA target sites for WT or deleted regions. Normalized data were calculated as ratios of Renilla/firefly luciferase intensities. The luminescence intensity significantly decreased upon co-transfection with miR-99a-3p and the vector carrying the wild-type sequences at positions 258-274 in the *RRM2* 3'-untranslated region. \* $P < 0.0001$ . (D) Spearman's correlation analysis revealed a negative correlation between *RRM2* expression and miR-99a-3p expression in The Cancer Genome Atlas ccRCC cohort ( $P = 0.001$ ;  $R = -0.189$ ). *RRM2*, ribonucleotide reductase regulatory subunit-M2; miR, microRNA; *GUSB*, glucuronidase  $\beta$ ; WT, wild type.

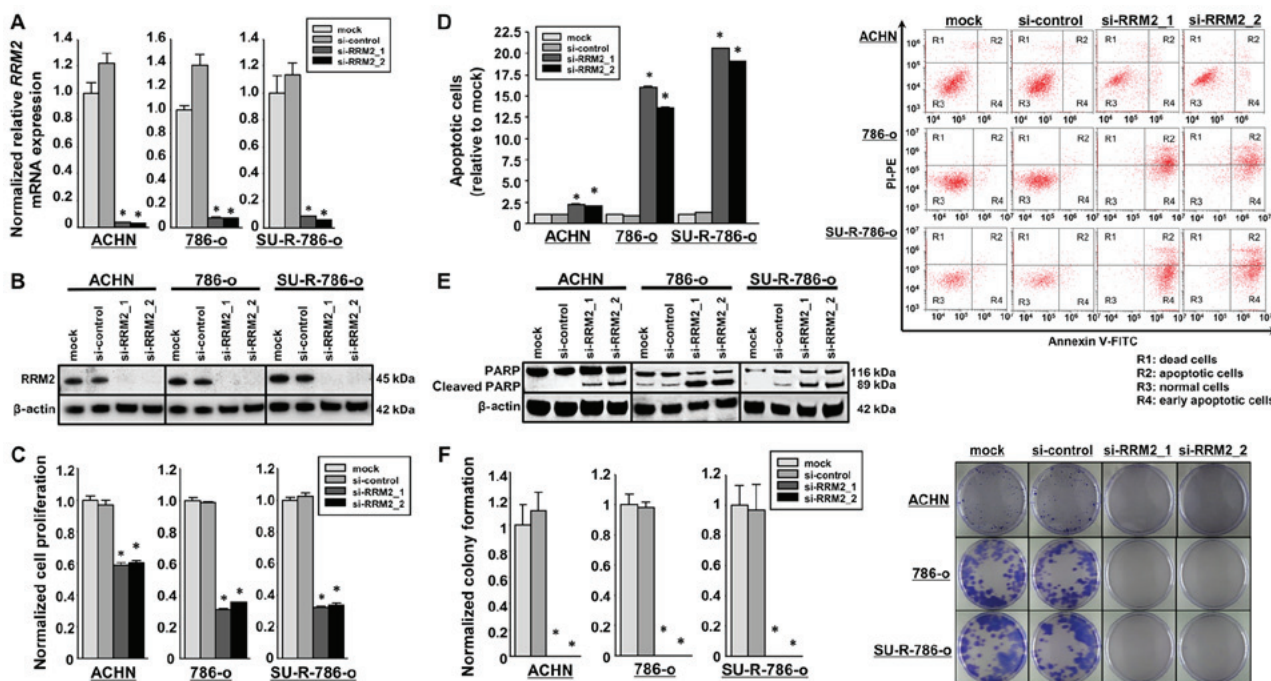


Figure 5. Effects of si-RRM2 transfection on SU-R-786-o, ACHN and 786-o cells. (A) The expression of *RRM2* mRNA was significantly inhibited in cells transfected with si-RRM2 compared with that in the mock and si-control groups. *GUSB* was employed as an internal control. \* $P < 0.0001$  versus mock and si-control groups. (B) The expression of *RRM2* protein, as observed by western blot analysis, was markedly inhibited in cells with si-RRM2 compared with that in the mock or si-control groups.  $\beta$ -actin was employed as a loading control. (C) Cell proliferation was examined using XTT assays in cells with *RRM2* knockdown, revealing a significant inhibition compared with the control groups. \* $P < 0.0001$ . (D) Apoptosis assays using flow cytometry indicated that the number of apoptotic cells was significantly greater in si-RRM2 transfectants than in the mock or siRNA-control transfection groups. \* $P < 0.0001$ . (E) Western blot analysis of apoptotic marker cleaved PARP in ACHN 786-o, and SU-R-786-o cells demonstrated a significant difference in cleaved PARP levels between cells with and without *RRM2* silencing.  $\beta$ -actin was employed as a loading control. (F) Colony formation assays demonstrated that colony growth was repressed in cells with *RRM2* knockdown compared with that in the mock or si-control groups. \* $P < 0.0001$ . si-, small interfering RNA; *RRM2*, ribonucleotide reductase regulatory subunit-M2; *GUSB*, glucuronidase  $\beta$ ; PARP, poly(ADP-ribose) polymerase; FITC, fluorescein isothiocyanate.



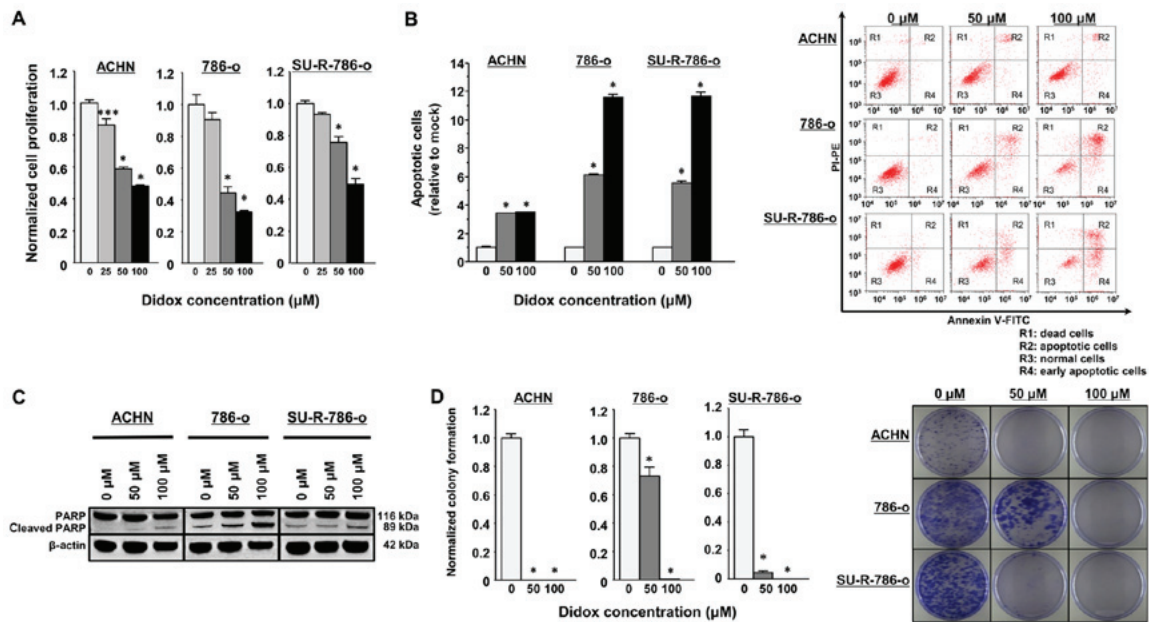


Figure 6. Effects of the ribonucleotide reductase regulatory subunit-M2 inhibitor Didox on SU-R-786-o, ACHN and 786-o cells. (A) Cell proliferation was determined by XTT assays using Didox concentrations of 25, 50 and 100  $\mu$ M, revealing a concentration-dependent inhibitory effect. \* $P < 0.0001$  and \*\*\* $P < 0.05$  versus no Didox. (B) Flow cytometry apoptosis assays indicated that the number of apoptotic cells was significantly greater following Didox treatment in a concentration-dependent manner. \* $P < 0.0001$  versus no Didox. (C) Western blot analysis of apoptotic marker cleaved PARP following Didox treatment in ACHN, 786-o and SU-R-786-o cells demonstrated an increase in cleaved PARP.  $\beta$ -actin was employed as a loading control. (D) The colony formation ability of cells was inhibited by Didox in a concentration-dependent manner. \* $P < 0.0001$  versus no Didox. PARP, poly (ADP-ribose) polymerase; FITC, fluorescein isothiocyanate.

indicated that high expression of *RRM2* is associated with oncogenic effects in ACHN, 786-o and SU-R-786-o cells.

**Effects of the *RRM2* inhibitor Didox on cell proliferation, apoptosis and colony formation in SU-R-786-o cells.** The above findings imply that *RRM2* inhibitors may be a promising anticancer agent for repressing cell proliferation and colony formation by enhancing apoptosis. Didox has strong inhibitory effects against ribonucleotide reductase that are associated with DNA synthesis and repair by blocking the synthesis of deoxyribonucleotides; this inhibitor has demonstrated strong antitumor effects (32-35). In preliminary analyses, the inhibition of *RRM2* by Didox (50 or 100  $\mu$ M) was demonstrated to significantly decrease the proliferation of SU-R-786-o, ACHN and parental 786-o cells (Fig. 6A). Apoptosis assays revealed that Didox had significant apoptotic effects in these cells ( $P < 0.0001$ ; Fig. 6B). Western blot analyses also revealed that the levels of cleaved PARP were markedly increased in cells treated with Didox in a concentration-dependent manner (Fig. 6C). In addition, 50 or 100  $\mu$ M Didox led to significant inhibition of colony formation of the cells in a concentration-dependent manner ( $P < 0.0001$ ; Fig. 6D). These data suggest that the *RRM2* inhibitor Didox may lead to anticancer effects by inhibiting cancer cell growth, promoting apoptosis and modulating the colony formation ability in SU-R-786-o and other RCC cells.

## Discussion

The guide-strand RNA derived from double-stranded miRNA is maintained for direct binding of the RNA-induced silencing complex to target mRNAs, whereas the

passenger-strand RNA is degraded (10,36). Although a previous study performed functional analyses of miR-99a (guide-strand) in RCC (37), miR-99a-3p (passenger-strand) was selected as a candidate miRNA and therapeutic target in RCC and SU-R-786-o cells in the present study. Recently, the two strands of pre-miR-145, miR-145-5p (guide-strand) and miR-145-3p (passenger-strand), have been reported to act as antitumor miRNAs in bladder cancer cells by regulating the gene encoding ubiquitin-like with PHD and ring finger domains 1 (23). In addition, the passenger strand miR-21-3p has been reported to mediate cisplatin resistance in ovarian cancer (38). Therefore, passenger-strand miRNAs may also be associated with resistance to chemotherapeutic agents. In fact, several other studies have reported on miRNAs involved in resistance to molecular-targeted agents in various cancer types (39,40). Yumioka *et al* (41) demonstrated that restoring miR-194-5p expression in sunitinib-resistant ccRCC cells sensitized to sunitinib by downregulating lysosome-associated membrane protein 2. On the other hand, Kishikawa *et al* (42) reported that decreased miR-122 expression may be involved in sorafenib sensitivity through the upregulation of solute carrier family 7 expression in hepatocellular carcinoma. The present study focused on miR-99a-3p due to the observation that this miRNA strongly inhibited the viability of 786-o and SU-R-786-o cells. Additionally, a trend towards shorter OS times in patients with low expression levels of miR-99a-3p was observed, but this was not statistically significant. Furthermore, cell function assays demonstrated that apoptosis was induced and colony formation was inhibited in ACHN, 786-o and SU-R-786-o cells transfected with this miRNA. To the best of our knowledge, no studies have revealed that passenger-strand miR-99a-3p is associated with

tumorigenesis in RCC. In other cancer types, miR-99a-3p has been reported to act as a tumor suppressor in naïve and castration-resistant prostate cancer (43). Additionally, miR-99a-3p was validated as a predictor of response to standard fluoropyrimidine-based chemotherapy in patients with metastatic colorectal cancer (44). Therefore, the present finding that miR-99a-3p acts as a tumor suppressor in RCC cells, including the SU-R-786-o, is reasonable, even though SU-R-786-o cells were the only sunitinib-resistant cell line used in this study. Therefore, additional studies are necessary to investigate the functional roles of miR-99a-3p and *RRM2* in more sunitinib-resistant RCC cell lines. In terms of the regulatory mechanisms of miR-99a-3p, this study attempted to explore how miR-99a-3p downregulation occurred in normal and sunitinib-resistant RCC. Based on the TCGA ccRCC cohort using the cBioPortal, genetic copy number alterations involving miR-99a-3p were revealed in only 0.2% of cases (1 out of 528 sequenced cases). Notably, no reports have suggested that miR-99a-3p is regulated epigenetically by DNA methylation, histone modification or noncoding RNAs in RCC or other cancer types. Future studies are necessary to elucidate the mechanisms of miR-99a-3p downregulation in normal and sunitinib-resistant RCC. In this study, the expression levels of miR-99a-3p were significantly lower than in normal kidney cell RNA, with the exception of the A498 cells. It is possible that the variation in the expression levels of miR-99a-3p in the various cell lines are due to their different clinical origins.

The *RRM2* protein is one of two subunits of the ribonucleotide reductase complex, catalyzing the formation of deoxyribonucleotides from ribonucleotides. Oncogenic roles of *RRM2* have been reported in several cancer types, including adrenocortical cancer, gastric adenocarcinoma, breast cancer and melanoma (45-48). In colorectal cancer and non-small cell lung carcinoma, *RRM2* upregulation was revealed to be associated with shorter survival time (49,50). Overexpression of *RRM2* has been reported to enhance the potential of cellular transformation by various oncogenes and to increase the malignant potential of transformed cells (51). However, to the best of our knowledge, this is the first study demonstrating the oncogenic role of *RRM2* in RCC as well as sunitinib-resistant RCC cells. Previous studies have demonstrated that *RRM2* knockdown causes S-phase arrest with no particular enrichment of the G<sub>1</sub>-phase population in ccRCC cell lines (52). However, no reports have described the effects of miR-99a-3p expression on the cell cycle. In the present study, cell cycle arrest was evaluated in miR-99a-3p- and si-*RRM2*-transfectants using flow cytometry and demonstrated that S-phase arrest was induced in the transfected 786-o cells. By contrast, in the SU-R-786-o cells, miR-99a-3p transfection caused S-phase arrest, whereas *RRM2* knockdown caused G<sub>0</sub>/G<sub>1</sub>-phase arrest. These results suggest that there are additional complex mechanisms mediated by *RRM2* that affect cell cycle arrest in sunitinib-resistant cells. Further studies are necessary to elucidate these mechanisms.

Malignant cells often exhibit a shift in cellular metabolism from oxidative phosphorylation to glycolysis, known as the Warburg effect (53,54). As the Warburg effect is considered a fundamental property of neoplasia, targeting glycolysis may be a therapeutically relevant strategy for cancer treatment (55).

In addition, a previous study demonstrated that the Warburg effect contributes to resistance to molecular-targeted agents in various cancer types (56). Previous studies have indicated that ccRCC exhibits increased glucose utilization as a result of overexpression of the genes encoding glucose transporter protein type 1 and hexokinase-2, known as glycolytic enzymes (57,24). In addition, it has also been demonstrated that metabolic reprogramming and chromatin remodeling occur in sunitinib-resistant cells (6). Notably, previous reports on cervical and breast cancer confirmed that *RRM2* overexpression specifically upregulates hypoxia-inducible factor (HIF)-1 $\alpha$ -associated proliferation and differentiation pathways and *VEGF* expression via the activation of the extracellular signal-regulated kinase 1/2 signaling pathway (58,59). As continuous HIF activation is thought to be critical for RCC progression and acquired resistance to tyrosine kinase inhibitors and mTOR inhibitors (60), the finding that *RRM2* was upregulated via miR-99a-3p downregulation in sunitinib-resistant cells may represent another mechanism through which RCC cells acquire sunitinib resistance. Indeed, several reports have confirmed that the upregulation of *RRM2* contributes to resistance to chemotherapeutic agents in various types of cancer (61-63). Therefore, further studies using *in vivo* models are required to elucidate the associations between angiogenesis and sunitinib resistance.

In summary, the present study demonstrated that miR-99a-3p was downregulated in several RCC cell lines and SU-R-786-o cells. Additionally, this miRNA was demonstrated to act as a tumor suppressor through regulating oncogenic *RRM2*. To the best of our knowledge, this is the first report to demonstrate that tumor-suppressive miR-99a-3p directly targets *RRM2*. The identification of novel molecular pathways and targets regulated by the miR-99a-3p/*RRM2* axis may improve our understanding of sunitinib-resistant RCC.

## Acknowledgements

The authors thank Ms. Mutsumi Miyazaki and Ms. Keiko Yoshitomi, Department of Urology, Graduate School of Medical and Dental Sciences, Kagoshima University (Kagoshima, Japan), for their excellent laboratory assistance.

## Funding

This study was supported by a Grant-in-Aid for Scientific Research from the Japan Society for the Promotion of Science, Tokyo, Japan (nos. 16H05464, 17H04332 and 16K11015).

## Availability of data and materials

All datasets used in this study are already provided as a part of the submitted article.

## Authors' contributions

YO, HY, MY, HE and MN conceived of the study and designed the experiments. YO, HY, TS and SS performed the experiments. YO, HY and HE drafted the manuscript. All authors reviewed the manuscript and approved the final version.

## Ethics approval and consent to participate

The present study was approved by the Bioethics Committee of Kagoshima University, and written informed consent and was obtained from all patients.

## Patient consent for publication

Not applicable.

## Competing interests

The authors declare no competing interests.

## References

- López JI: Renal tumors with clear cells. A review. *Pathol Res Pract* 209: 137-146, 2013.
- Ohba K, Miyata Y, Yasuda T, Asai A, Mitsunari K, Matsuo T, Mochizuki Y, Matsunaga N and Sakai H: Efficacy and safety of sunitinib alternate day regimen in patients with metastatic renal cell carcinoma in Japan: Comparison with standard 4/2 schedule. *Asia Pac J Clin Oncol* 14: 153-158, 2018.
- Yang F, Zhou X, Du S, Zhao Y, Ren W, Deng Q, Wang F and Yuan J: LIM and SH3 domain protein 1 (LASP-1) overexpression was associated with aggressive phenotype and poor prognosis in clear cell renal cell cancer. *PLoS One* 9: e100557, 2014.
- Teng J, Gao Y, Chen M, Wang K, Cui X, Liu Y and Xu D: Prognostic value of clinical and pathological factors for surgically treated localized clear cell renal cell carcinoma. *Chin Med J (Engl)* 127: 1640-1644, 2014.
- Bergers G and Hanahan D: Modes of resistance to anti-angiogenic therapy. *Nat Rev Cancer* 8: 592-603, 2008.
- Yoshino H, Nohata N, Miyamoto K, Yonemori M, Sakaguchi T, Sugita S, Itesako T, Kofuji S, Nakagawa M, Dahiya R, *et al*: PHGDH as a key enzyme for serine biosynthesis in HIF2alpha targeting therapy for renal cell carcinoma. *Cancer Res* 77: 6321-6329, 2017.
- Rajan A, Kim C, Heery CR, Guha U and Gulley JL: Nivolumab, anti-programmed death-1 (PD-1) monoclonal antibody immunotherapy: Role in advanced cancers. *Hum Vaccin Immunother* 12: 2219-2231, 2016.
- Motzer RJ, Escudier B, McDermott DF, George S, Hammers HJ, Srinivas S, Tykodi SS, Sosman JA, Procopio G, Plimack ER, *et al*: CheckMate 025 Investigators: Nivolumab versus Everolimus in Advanced Renal-Cell Carcinoma. *N Engl J Med* 373: 1803-1813, 2015.
- Sarfaty M, Leshno M, Gordon N, Moore A, Neiman V, Rosenbaum E and Goldstein DA: Cost Effectiveness of Nivolumab in Advanced Renal Cell Carcinoma. *Eur Urol* 73: 628-634, 2018.
- Carthew RW and Sontheimer EJ: Origins and Mechanisms of miRNAs and siRNAs. *Cell* 136: 642-655, 2009.
- Landgraf P, Rusu M, Sheridan R, Sewer A, Iovino N, Aravin A, Pfeffer S, Rice A, Kamphorst AO, Landthaler M, *et al*: A mammalian microRNA expression atlas based on small RNA library sequencing. *Cell* 129: 1401-1414, 2007.
- Kozomara A and Griffiths-Jones S: miRBase: Integrating microRNA annotation and deep-sequencing data. *Nucleic Acids Res* 39 (Database): D152-D157, 2011.
- Kawakami K, Enokida H, Chiyomaru T, Tatarano S, Yoshino H, Kagura I, Gotanda T, Tachiwada T, Nishiyama K, Nohata N, *et al*: The functional significance of miR-1 and miR-133a in renal cell carcinoma. *Eur J Cancer* 48: 827-836, 2012.
- Xie M, Dart DA, Guo T, Xing XF, Cheng XJ, Du H, Jiang WG, Wen XZ and Ji JF: MicroRNA-1 acts as a tumor suppressor microRNA by inhibiting angiogenesis-related growth factors in human gastric cancer. *Gastric cancer* 21: 41-54, 2018.
- Xu W, Zhang Z, Zou K, Cheng Y, Yang M, Chen H, Wang H, Zhao J, Chen P, He L, *et al*: MiR-1 suppresses tumor cell proliferation in colorectal cancer by inhibition of Smad3-mediated tumor glycolysis. *Cell Death Dis* 8: e2761, 2017.
- Xi Y: MicroRNA: A New Player for Cancer Chemoprevention. *J Integr Oncol* 2: pii: 105, 2013.
- Yi B, Piazza GA, Su X and Xi Y: MicroRNA and cancer chemoprevention. *Cancer Prev Res (Phila)* 6: 401-409, 2013.
- Lin HM, Nikolic I, Yang J, Castillo L, Deng N, Chan CL, Yeung NK, Dodson E, Elsworth B, Spielman C, *et al*: MicroRNAs as potential therapeutics to enhance chemosensitivity in advanced prostate cancer. *Sci Rep* 8: 7820, 2018.
- Xiao W, Lou N, Ruan H, Bao L, Xiong Z, Yuan C, Tong J, Xu G, Zhou Y, Qu Y, *et al*: Mir-144-3p Promotes Cell Proliferation, Metastasis, Sunitinib Resistance in Clear Cell Renal Cell Carcinoma by Downregulating ARID1A. *Cell Physiol Biochem* 43: 2420-2433, 2017.
- Sobin LH and Compton CC: TNM seventh edition: what's new, what's changed: communication from the International Union Against Cancer and the American Joint Committee on Cancer. *Cancer* 116: 5336-5339, 2010.
- Livak KJ and Schmittgen TD: Analysis of relative gene expression data using real-time quantitative PCR and the 2(-Delta Delta C(T)) method. *Methods* 25: 402-408, 2001.
- Ichimi T, Enokida H, Okuno Y, Kunimoto R, Chiyomaru T, Kawamoto K, Kawahara K, Toki K, Kawakami K, Nishiyama K, *et al*: Identification of novel microRNA targets based on microRNA signatures in bladder cancer. *Int J Cancer* 125: 345-352, 2009.
- Matsushita R, Yoshino H, Enokida H, Goto Y, Miyamoto K, Yonemori M, Inoguchi S, Nakagawa M and Seki N: Regulation of UHRF1 by dual-strand tumor-suppressor microRNA-145 (miR-145-5p and miR-145-3p): Inhibition of bladder cancer cell aggressiveness. *Oncotarget* 7: 28460-28487, 2016.
- Yoshino H, Enokida H, Itesako T, Kojima S, Kinoshita T, Tatarano S, Chiyomaru T, Nakagawa M and Seki N: Tumor-suppressive microRNA-143/145 cluster targets hexokinase-2 in renal cell carcinoma. *Cancer Sci* 104: 1567-1574, 2013.
- Bradford MM: A rapid and sensitive method for the quantitation of microgram quantities of protein utilizing the principle of protein-dye binding. *Anal Biochem* 72: 248-254, 1976.
- Yoshino H, Chiyomaru T, Enokida H, Kawakami K, Tatarano S, Nishiyama K, Nohata N, Seki N and Nakagawa M: The tumour-suppressive function of miR-1 and miR-133a targeting TAGLN2 in bladder cancer. *Br J Cancer* 104: 808-818, 2011.
- Anaya J: OncoLnc: linking TCGA survival data to mRNAs, miRNAs, and lncRNAs. *PeerJ Computer Science* 2: e67, 2016.
- Berkers J, Govaere O, Wolter P, Beuselinck B, Schöffski P, van Kempen LC, Albersen M, Van den Oord J, Roskams T, Swinnen J, *et al*: A possible role for microRNA-141 down-regulation in sunitinib resistant metastatic clear cell renal cell carcinoma through induction of epithelial-to-mesenchymal transition and hypoxia resistance. *J Urol* 189: 1930-1938, 2013.
- Papadopoulos EI, Yousef GM and Scorilas A: Cytotoxic activity of sunitinib and everolimus in Caki-1 renal cancer cells is accompanied by modulations in the expression of apoptosis-related microRNA clusters and BCL2 family genes. *Biomed Pharmacother* 70: 33-40, 2015.
- Goto Y, Kurozumi A, Nohata N, Kojima S, Matsushita R, Yoshino H, Yamazaki K, Ishida Y, Ichikawa T, Naya Y, *et al*: The microRNA signature of patients with sunitinib failure: Regulation of UHRF1 pathways by microRNA-101 in renal cell carcinoma. *Oncotarget* 7: 59070-59086, 2016.
- Merhautova J, Hezova R, Poprach A, Kovarikova A, Radova L, Svoboda M, Vyzula R, Demlova R and Slaby O: miR-155 and miR-484 Are Associated with Time to Progression in Metastatic Renal Cell Carcinoma Treated with Sunitinib. *BioMed Res Int* 2015: 941980, 2015.
- Elford HL, Freese M, Passamani E and Morris HP: Ribonucleotide reductase and cell proliferation. I. Variations of ribonucleotide reductase activity with tumor growth rate in a series of rat hepatomas. *J Biol Chem* 245: 5228-5233, 1970.
- Elford HL, Wampler GL and van't Riet B: New ribonucleotide reductase inhibitors with antineoplastic activity. *Cancer Res* 39: 844-851, 1979.
- Elford HL, Van't Riet B, Wampler GL, Lin AL and Elford RM: Regulation of ribonucleotide reductase in mammalian cells by chemotherapeutic agents. *Adv Enzyme Regul* 19: 151-168, 1980.
- van't Riet B, Wampler GL and Elford HL: Synthesis of hydroxy- and amino-substituted benzohydroxamic acids: Inhibition of ribonucleotide reductase and antitumor activity. *J Med Chem* 22: 589-592, 1979.
- Chendrimada TP, Finn KJ, Ji X, Baillat D, Gregory RI, Liebhaber SA, Pasquinelli AE and Shiekhattar R: MicroRNA silencing through RISC recruitment of eIF6. *Nature* 447: 823-828, 2007.



37. Cui L, Zhou H, Zhao H, Zhou Y, Xu R, Xu X, Zheng L, Xue Z, Xia W, Zhang B, *et al*: MicroRNA-99a induces G1-phase cell cycle arrest and suppresses tumorigenicity in renal cell carcinoma. *BMC Cancer* 12: 546, 2012.
38. Pink RC, Samuel P, Massa D, Caley DP, Brooks SA and Carter DR: The passenger strand, miR-21-3p, plays a role in mediating cisplatin resistance in ovarian cancer cells. *Gynecol Oncol* 137: 143-151, 2015.
39. Ayers D and Vandesompele J: Influence of microRNAs and Long Non-Coding RNAs in Cancer Chemoresistance. *Genes (Basel)* 8: 8, 2017.
40. An X, Sarmiento C, Tan T and Zhu H: Regulation of multidrug resistance by microRNAs in anti-cancer therapy. *Acta Pharm Sin B* 7: 38-51, 2017.
41. Yumioka T, Osaki M, Sasaki R, Yamaguchi N, Onuma K, Iwamoto H, Morizane S, Honda M, Takenaka A and Okada F: Lysosome-associated membrane protein 2 (LAMP-2) expression induced by miR-194-5p downregulation contributes to sunitinib resistance in human renal cell carcinoma cells. *Oncol Lett* 15: 893-900, 2018.
42. Kishikawa T, Otsuka M, Tan PS, Ohno M, Sun X, Yoshikawa T, Shibata C, Takata A, Kojima K, Takehana K, *et al*: Decreased miR122 in hepatocellular carcinoma leads to chemoresistance with increased arginine. *Oncotarget* 6: 8339-8352, 2015.
43. Arai T, Okato A, Yamada Y, Sugawara S, Kurozumi A, Kojima S, Yamazaki K, Naya Y, Ichikawa T and Seki N: Regulation of NCAPG by miR-99a-3p (passenger strand) inhibits cancer cell aggressiveness and is involved in CRPC. *Cancer Med* 7: 1988-2002, 2018.
44. Molina-Pinelo S, Carnero A, Rivera F, Estevez-Garcia P, Bozada JM, Limon ML, Benavent M, Gomez J, Pastor MD, Chaves M, *et al*: MiR-107 and miR-99a-3p predict chemotherapy response in patients with advanced colorectal cancer. *BMC Cancer* 14: 656, 2014.
45. Grolmusz VK, Karász K, Micsik T, Tóth EA, Mészáros K, Karvaly G, Barna G, Szabó PM, Baghy K, Matkó J, *et al*: Cell cycle dependent RRM2 may serve as proliferation marker and pharmaceutical target in adrenocortical cancer. *Am J Cancer Res* 6: 2041-2053, 2016.
46. Kang W, Tong JH, Chan AW, Zhao J, Wang S, Dong Y, Sin FM, Yeung S, Cheng AS, Yu J, *et al*: Targeting ribonucleotide reductase M2 subunit by small interfering RNA exerts anti-oncogenic effects in gastric adenocarcinoma. *Oncol Rep* 31: 2579-2586, 2014.
47. Shah KN, Mehta KR, Peterson D, Evangelista M, Livesey JC and Faridi JS: AKT-induced tamoxifen resistance is overturned by RRM2 inhibition. *Mol Cancer Res* 12: 394-407, 2014.
48. Zuckerman JE, Hsueh T, Koya RC, Davis ME and Ribas A: siRNA knockdown of ribonucleotide reductase inhibits melanoma cell line proliferation alone or synergistically with temozolomide. *J Invest Dermatol* 131: 453-460, 2011.
49. Liu X, Zhang H, Lai L, Wang X, Loera S, Xue L, He H, Zhang K, Hu S, Huang Y, *et al*: Ribonucleotide reductase small subunit M2 serves as a prognostic biomarker and predicts poor survival of colorectal cancers. *Clin Sci (Lond)* 124: 567-578, 2013.
50. Mah V, Alavi M, Márquez-Garbán DC, Maresh EL, Kim SR, Horvath S, Bagryanova L, Huerta-Yepez S, Chia D, Pietras R, *et al*: Ribonucleotide reductase subunit M2 predicts survival in subgroups of patients with non-small cell lung carcinoma: Effects of gender and smoking status. *PLoS One* 10: e0127600, 2015.
51. Fan H, Villegas C and Wright JA: Ribonucleotide reductase R2 component is a novel malignancy determinant that cooperates with activated oncogenes to determine transformation and malignant potential. *Proc Natl Acad Sci USA* 93: 14036-14040, 1996.
52. Avolio TM, Lee Y, Feng N, Xiong K, Jin H, Wang M, Vassilakos A, Wright J and Young A: RNA interference targeting the R2 subunit of ribonucleotide reductase inhibits growth of tumor cells in vitro and in vivo. *Anticancer Drugs* 18: 377-388, 2007.
53. Kroemer G and Pouyssegur J: Tumor cell metabolism: Cancer's Achilles' heel. *Cancer Cell* 13: 472-482, 2008.
54. Vander Heiden MG: Targeting cancer metabolism: A therapeutic window opens. *Nat Rev Drug Discov* 10: 671-684, 2011.
55. Lai IL, Chou CC, Lai PT, Fang CS, Shirley LA, Yan R, Mo X, Bloomston M, Kulp SK, Bekaii-Saab T, *et al*: Targeting the Warburg effect with a novel glucose transporter inhibitor to overcome gemcitabine resistance in pancreatic cancer cells. *Carcinogenesis* 35: 2203-2213, 2014.
56. Liu J, Pan C, Guo L, Wu M, Guo J, Peng S, Wu Q and Zuo Q: A new mechanism of trastuzumab resistance in gastric cancer: MACC1 promotes the Warburg effect via activation of the PI3K/AKT signaling pathway. *J Hematol Oncol* 9: 76, 2016.
57. Yamasaki T, Seki N, Yoshino H, Itesako T, Yamada Y, Tatarano S, Hidaka H, Yonezawa T, Nakagawa M and Enokida H: Tumor-suppressive microRNA-1291 directly regulates glucose transporter 1 in renal cell carcinoma. *Cancer Sci* 104: 1411-1419, 2013.
58. Wang N, Zhan T, Ke T, Huang X, Ke D, Wang Q and Li H: Increased expression of RRM2 by human papillomavirus E7 oncoprotein promotes angiogenesis in cervical cancer. *Br J Cancer* 110: 1034-1044, 2014.
59. Shah KN, Wilson EA, Malla R, Elford HL and Faridi JS: Targeting Ribonucleotide Reductase M2 and NF- $\kappa$ B Activation with Didox to Circumvent Tamoxifen Resistance in Breast Cancer. *Mol Cancer Ther* 14: 2411-2421, 2015.
60. Rini BI and Atkins MB: Resistance to targeted therapy in renal-cell carcinoma. *Lancet Oncol* 10: 992-1000, 2009.
61. Putluri N, Maity S, Kommagani R, Creighton CJ, Putluri V, Chen F, Nanda S, Bhowmik SK, Terunuma A, Dorsey T, *et al*: Pathway-centric integrative analysis identifies RRM2 as a prognostic marker in breast cancer associated with poor survival and tamoxifen resistance. *Neoplasia* 16: 390-402, 2014.
62. Zhou B, Su L, Hu S, Hu W, Yip ML, Wu J, Gaur S, Smith DL, Yuan YC, Synold TW, *et al*: A small-molecule blocking ribonucleotide reductase holoenzyme formation inhibits cancer cell growth and overcomes drug resistance. *Cancer Res* 73: 6484-6493, 2013.
63. Zhang M, Wang J, Yao R and Wang L: Small interfering RNA (siRNA)-mediated silencing of the M2 subunit of ribonucleotide reductase: a novel therapeutic strategy in ovarian cancer. *Int J Gynecol Cancer* 23: 659-666, 2013.